Int. J. Electrochem. Sci., 15 **(2020)** 7053 – 7063, doi: 10.20964/2020.07.90

International Journal of
ELECTROCHEMICAL
SCIENCE
www.electrochemsci.org

Synthesis of $MnMoO_4$ Nanorods by a Simple Co-Precipitation Method in Presence of Polyethylene Glycol for Pseudocapacitor Application

Sivakumar Musuvadhi Babulal[1], *Krishnan Venkatesh*[2], *Tse-Wei Chen*[3], *Shen-Ming Chen*[1,*] *Alagumalai Krishnapandi*[1], *Syang-Peng Rwei*[4,5], *and Sayee Kannan Ramaraj*[2,*]

[1] Electroanalysis and Biotelectrochemistry Lab, Department of Chemical Engineering and Biotechnology, National Taipei University of Technology, No.1, Section 3, Chung-Hsiao East Road, Taipei 106, Taiwan R.O.C.
[2] Thiagarajar College (Autonomous), Madurai, Tamil Nadu, India.
[3]Department of Materials, Imperial College London, London, SW7 2AZ, United Kingdom
[4]Research and Development Center for Smart Textile Technology, National Taipei University of Technology, Taiwan
[5]Institute of Organic and Polymeric Materials, National Taipei University of Technology, Taiwan
[*]E-mail: smchen78@ms15.hinet.net; sayeekannanramaraj@gmail.com

Received: 3 April 2020 / *Accepted:* 27 May 2020 / *Published:* 10 June 2020

Recent attention has focused on the synthesis and application of the binary oxide-based nanomaterial, which can have superior electrochemical performance than the single oxide materials. The metal molybdate has drawn significant attention due to its multiple oxidation states of molybdenum ion and its large electrical activity has been extensively studied in energy storage application. Here, we synthesized $MnMoO_4$ nanorods through the co-precipitation method with the aid of the polyethylene glycol (PEG) surfactant and its electrochemical properties are investigated toward the supercapacitor application. The crystalline structure and surface morphology of PEG-$MnMoO_4$ are evaluated by X-ray diffraction, Raman, field emission scanning electron microscope and elemental mapping, reveals the as-prepared PEG-$MnMoO_4$ exhibits uniform nanorods or forefinger-like morphology with monoclinic phase crystal structure. The as-fabricated PEG-$MnMoO_4$ nanorods electrode showed very high discharge capacity 424 F g^{-1} at a current density of 1 A g^{-1} with a large potential window 1.8 V vs. Ag/AgCl in 1 M Na_2SO_4. Hence, the surfactant-assisted synthesis of $MnMoO_4$ nanorods can be the best energy storage material that can deliver higher specific discharge capacity when it's combined with suitable supporting matrices.

Keywords: Co-precipitation method; Manganese molybdate; Pseudo capacitive materials; Binary transition metal oxide.

1. INTRODUCTION

In recent years, an increasing demands for energy storage system including electronic devices and electric vehicles that requires high power density with long cycle life [1,2]. Electrochemical capacitors can fulfil their requirements which exhibits a desirable properties such as high-power density, rapid charging ability with long cycle life, small size and low mass[3-5]. These electrochemical capacitors can be classified into two types based on their charge storage mechanism i.e., electrical double layer capacitor (EDLC) and pseudocapacitor. Non-faradic charge storage mechanism is occurred in EDLC electrode and electrolyte interfaces, it was commonly fabricated with porous and high surface area carbon based materials [6,7]. On the other hand, faradaic charge storage mechanism occurred on the pseudocapacitive electrode materials where it can exist as a reversible redox reaction for the charge storage. That redox reaction is specifically derived from the transition metal oxides and conducting polymers based materials. Up to now, a large number of supercapacitor devices have been commercialized using high surface area carbonaceous material due to its low cost and more abundant. However, their durability is limited due to the swelling or shrinking of the carbon materials during the charge-discharge cycling time. Hence, the pseudocapacitor development has currently paid much attention and must be used high abundant and low cost materials [1,2,8].

Transition metal oxides with various valence states are acquired more pseudocapacitive behavior for charge storage, among them ruthenium oxides are most widely explored theoretically and practically due to its high pseudocapacitance [9,10]. For the past few years, researchers have been focused on numerous low cost and high abundant materials such as Co_3O_4, NiO, MnO_2, and MoO_3 for pseudocapacitor application. These materials have an excellent catalytic and electrochemical activity and possess higher specific capacitance [11-14]. Recently, metal molybdate ($MMoO_4$; M = Ni, Mn, Co, Ce, Ag, Sn, Cu, Ca, Mg, etc.) have aroused tremendous research interest due to their low cost, abundant resource and high electrochemical activity [15-21]. In particular, manganese molybdate ($MnMoO_4$), which holds various oxidation states of Mn and Mo in $MnMoO_4$ phase, delivers high specific capacity owing to its mixed valence states that can tune the charge storage property of the materials [22-28]. Mai et al [4] synthesized a three-dimensional $MnMoO_4/CoMoO_4$ hybrid materials for supercapacitor, displays the specific discharge capacity around 187.1 F g^{-1} at 1 A g^{-1}. Gosh et al [27] had synthesized a three dimensional hexahedron shaped α-$MnMoO_4$ by hydrothermal method for high energy density supercapacitor electrode which exhibits the specific capacity of 234 F g^{-1} at 2 A g^{-1} in a wide potential range 2 V in 1 M Na_2SO_4 electrolyte system. Jesuraj et al [28] had also reported one dimensional porous α-$MnMoO_4$ nanorods by sonochemical synthesis method, the capacitive performance was displayed at 1 V potential range in 1 M Na_2SO_4 which delivers the specific capacity of 373 F g^{-1} at 1 A g^{-1}.

In this work, we have synthesized $MnMoO_4$ nanorods as an efficient pseudocapacitive electrode material via simple co-precipitation method with adding polyethylene glycol (PEG) as a surfactant to improve the crystallinity and phase purity of the binary oxides. The as-synthesized PEG-$MnMoO_4$ nanorods exhibit a large potential window (1.8 V vs. Ag/AgCl) in neutral pH electrolyte (1 M Na_2SO_4) to obtain the higher specific discharge capacity 424 F g^{-1} at 1 A g^{-1}. Thus, the proposed synthesis strategy can be a simple and scalable for the preparation of binary metal oxide and it can be used to fabricate the energy storage devices.

2. EXPERIMENTAL

2.1. Materials and methods

All chemical is of analytical grade and used as received without any further purification. Sodium molybdate dihydrate ($Na_2MoO_4.2H_2O$), Manganese chloride tetrahydrate ($MnCl_2.4H_2O$), and sodium sulphate (Na_2SO_4), porous super P, polyvinylidene difluoride (PVDF), N-methyl-2-pyrrolidone (NMP) and polyethylene glycol (PEG) were received from Sigma-Aldrich chemicals.

2.2 Synthesis of $MnMoO_4$ nanorods

$MnMoO_4$ nanorods are synthesized by simple co-precipitation method by adding transition metal precursors with PEG surfactant at room temperature. Prior to synthesis process, 0.05 M $MnCl_2.4H_2O$ and 0.1 M $NaMoO_4.2H_2O$ aqueous solutions were separately prepared in 30 mL de-ionized (DI) water under stirring for 10 min. Later, $NaMoO_4$ solution was added drop by drop into the homogenous $MnCl_2$ solution. Simultaneously, 10 mL of PEG solution was added to that above mixture and stirred at room temperature for 3 h to obtain the complete precipitates. The precipitates were collected by vacuum filtration and washed several times with DI water and absolute ethanol to remove the unreacted impurities. The obtained product was dried at 80 °C for 12 h and calcined at 600 °C for 3 h in air, the final resulted product was named as PEG-$MnMoO_4$ nanorods. For comparison, $MnMoO_4$ nanorods were synthesized by same experimental condition without adding PEG surfactant. The detailed synthesis process was displayed in **Scheme 1**. The following mechanism reveals the successful formation of $MnMoO_4$ (see equation (1) – (4));

$$MnCl_2.4H_2O \rightarrow Mn^{2+} + 2Cl^- \quad (1)$$

$$NaMoO_4.2H_2O \rightarrow 2Na^+ + MoO_4^{2-} \quad (2)$$

$$Mn^{2+} + MoO_4^{2-} \rightarrow MnMoO_4.xH_2O \quad (3)$$

$$MnMoO_4.xH_2O \rightarrow MnMoO_4 \quad (4)$$

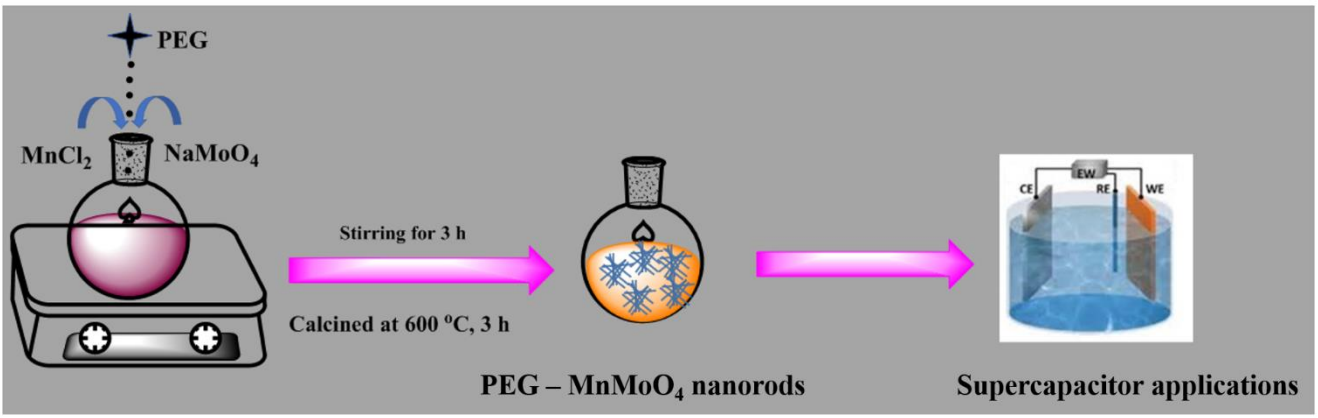

Scheme 1. Schematic illustration of the synthesis of PEG-$MnMoO_4$ nanorods.

2.3. Characterization

The crystal structure of $MnMoO_4$ nanorods was examined using X-ray powder diffraction (XRD: BRUKER D2 PHASER, Germany) with Cu Kα radiation source and Raman spectroscopy (confocal micro- Renishaw, 632 nm, He-Ne laser source, USA). The morphology of the pristine $MnMoO_4$ nanorods was examined by field emission scanning electron microscope (FE-SEM: JEOL JSM-7610F Plus, Japan) integrated with energy dispersive X-ray spectroscopy (EDS: Oxford X-MaxN, UK). The Fourier transform infrared spectroscopy (FT-IR) was recorded using Shimadzu FT-IR-8201PC instrument. The electrochemical measurement was evaluated cyclic voltammetry (CV), and chronopotentiometry using CHI 405 (CH Instruments, USA).

2.4. Electrode fabrication

To fabricate the pseudocapacitive electrode, the coating slurry was initially prepared by mixing the as-synthesized $MnMoO_4$ powders, porous super P and PVDF binder with a mass ratio of 80:10:10 in small amount of NMP solvent and grind well for 30 min. For the electrode material coating, nickel (Ni) foam was cut into small pieces (2 × 4 cm) and then cleaned the buffer layer on the Ni foam surface using 3 M HCl for 15 min followed by washing with DI water and ethanol several times. Then, the electrode material slurry was coated on the Ni foam (area of coating 1 cm^2) surface using painting brush and dried at 80 °C for 24 h. A three-electrode system were used to study the pseudocapacitive properties of the materials, the system was composed with $MnMoO_4$ nanorods coated Ni foam, Pt wire, and Ag/AgCl (saturated KCl) electrode as working, counter and reference electrodes, respectively. This integrated system was performed in 1 M Na_2SO_4 neutral aqueous electrolyte at room temperature. The electrochemical performances of the $MnMoO_4$ nanorods were investigated by CV and Galvanostatic charge/discharge (GCD) analysis.

3. RESULTS AND DISCUSSION

3.1 Materials characterization

Fig. 1 shows the FESEM images and EDS mapping of the as-synthesized PEG-$MnMoO_4$ electrode materials. Low and high magnification FESEM images (Fig. 1a & b) reveals the uniform and smooth surface of the nanorods or forefinger-like morphology with an average diameter and length of the nanorods are 160 nm and 2.3 µm, respectively. In order to study the chemical composition, EDS mapping and elemental analysis were performed to PEG-$MnMoO_4$ nanorods samples (Fig. 1c-f). It was found that the bright spots on selected area of the samples indicates the presence of Mn, Mo, and O elements. Also, the EDS spectra reveals the existence of Mn, Mo and O elements on the synthesized materials without any other impurities. The results clearly confirmed that the as-formed materials are $MnMoO_4$ with nanorods as well as forefinger-like morphology. Hence, these attractive nanostructure possess easy way to transport the ions resulting in enhanced electrochemical performance.

Crystallinity of PEG-$MnMoO_4$ nanorods was determined by XRD analysis. As shown in Fig. 2a, all the diffraction peaks are clearly indexed to the monoclinic phase of $MnMoO_4$ (JCPDS card No.06-0505). The individual peaks at 2θ angles are obtained to 13.14°, 19.03°, 23.10°, 25.05°, 26.18°, 27.02°, 28.15°, 31.36°, 32.36°, 33.47°, 37.96°, 39.22°, 40.77°, 42.72°, 44.56°, 45.95°, 46.79°, 51.56°, 52.26°, 53.10°, 55.21°, 58.44°, 59.82° and 63.33° which are assigned to (110), (020), (021), (201), (220), (221), (311), (202), (112), (022), (222), (400), (040), (132), (-222), (322), (113), (241), (204), (531), (440), (442), (024), (020), planes of monoclinic $MnMoO_4$ with the space group of C2/m, respectively. No impurity phases were found in the spectra, confirms the purity of the samples. Though, the crystallite size of the PEG-$MnMoO_4$ nanorod was calculated by Debye-Scherer formula [3] using the high intensity plane of (220), it was measured to be 26 nm.

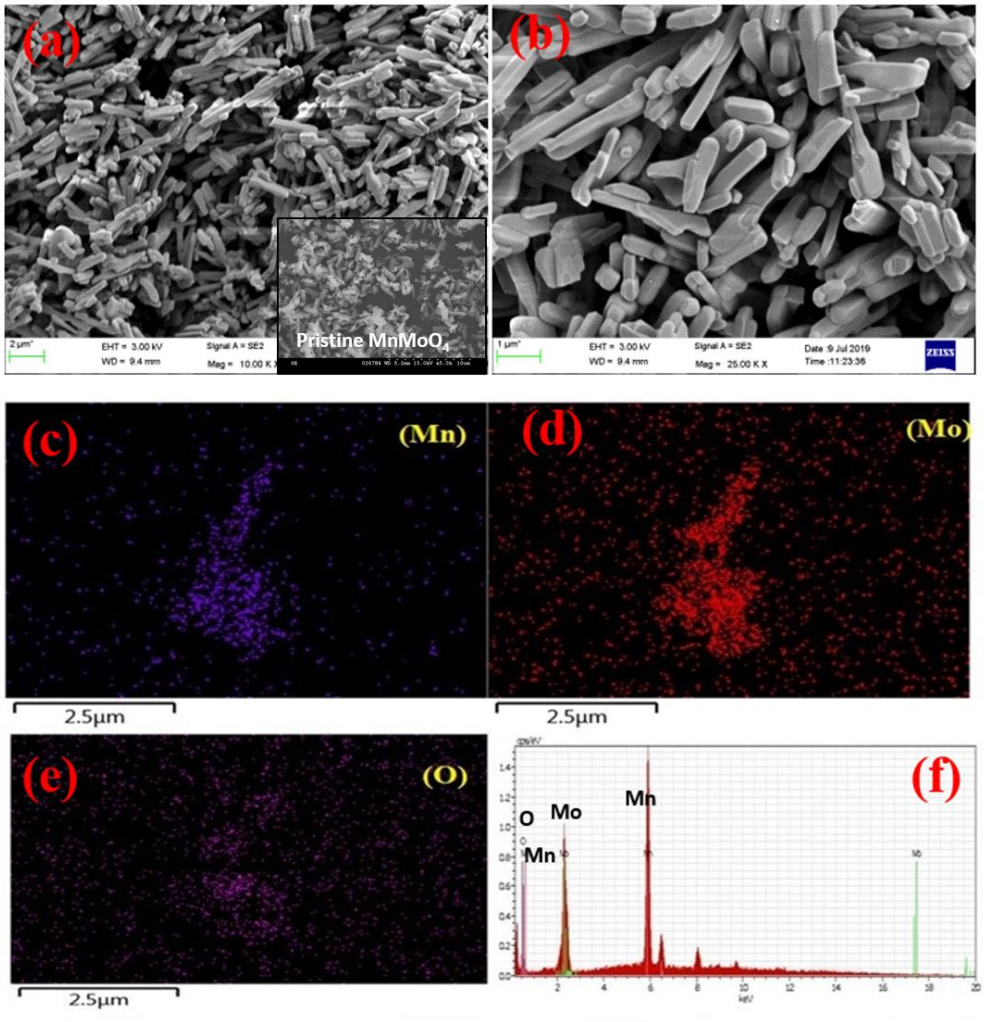

Figure 1. Low (a) and high (b) magnification FESEM images of PEG-$MnMoO_4$ nanorods. Inset of (a) FESEM image of pristine MnMoO4 nanorods. (c-e) EDS mapping analysis of PEG-$MnMoO_4$ nanorods. (f) EDS data of PEG-$MnMoO_4$ nanorods.

To the structural characteristics of the as-prepared PEG-$MnMoO_4$ nanorods were investigated by Raman spectroscopy (Fig. 2b). Usually, there are thirteen possible Raman active modes for $MnMoO_4$ monoclinic phase, such as $3A_g + 5B_g + 5E_g$. The strong high intense peak appearing at 926 and 817 cm^-

[1] is assigned symmetric vibration frequencies of Mo(1)O(2) and Mo(1)O(1) symmetric stretching vibration of $MnMoO_4$. The small intense peak at 351 cm^{-1} can be attributed to the A_g mode vibration of Mo–O group in $MnMoO_4$ [22]. Hence, the Raman spectra of PEG-$MnMoO_4$ nanorods clearly shows the material has obtained without any other crystalline phase change and defects.

FTIR study was used to further confirm the crystal structure and phase purity of the as-synthesized PEG-$MnMoO_4$ nanorods (Fig. 2c). FTIR spectra shows four intense characteristic IR bands at 721, 802, 866 and 947 cm^{-1}. All these major peaks are appeared below 1000 cm^{-1} wavenumber, assigned to the binding of metal and oxygen bond. These broad absorption bands were attributed to the Mo-O-Mo symmetric stretching vibrations of $MnMoO_4$, indicates the absence of hydroxyl and organic matters. From this spectra, the stretching vibration band appeared at 947 cm^{-1} corresponds to Mo=O group, whereas the bending vibration band at 866 cm^{-1} relates the Mo-O-Mo bond formation in $MnMoO_4$ [22,26]. The observed strong bands are confirmed the oxygen atoms are tetrahedrally coordinated with Mo atom on the unit cell of $MnMoO_4$.

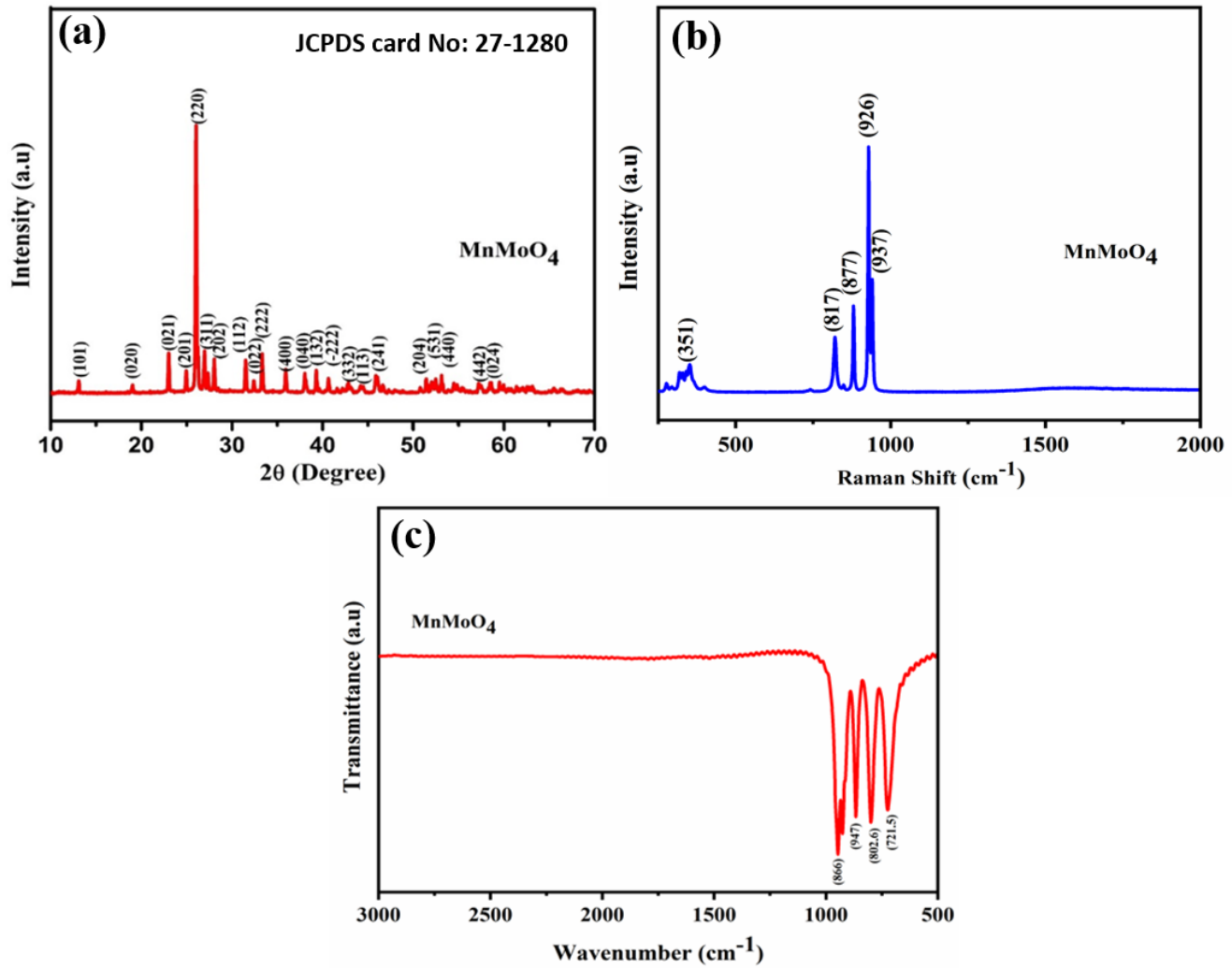

Figure 2. (a) XRD, (b) Raman and (c) FTIR analysis of PEG-$MnMoO_4$ nanorods.

3.2 Electrochemical performance of PEG-$MnMoO_4$ nanorods

The electrochemical behavior of PEG-$MnMoO_4$ nanorods coated Ni-foam electrode was examined using CV and GCD analysis. For optimization, initially, we compare the electrochemical activity of $MnMoO_4$ nanorods based on the effect of adding PEG surfactant in the synthesis. Fig. 3a & b shows the CV and GCD curves of PEG-$MnMoO_4$ and $MnMoO_4$ nanorods coated Ni-foam electrodes to observe the charge storage property. The CV scan was performed at the potential window of -1.0 to +1.0 V vs. Ag/AgCl in 1 M Na_2SO_4 electrolyte at a scan rate of 50 mV s^{-1}. A larger storage capacitive window was observed on PEG-$MnMoO_4$ coated Ni-foam electrode (-0.8 to +1.0 V) than the $MnMoO_4$ Ni-foam electrode (-0.4 to +1.0 V), indicates the higher charge storage behavior of the PEG assisted $MnMoO_4$ nanorods. In addition to GCD analysis, the PEG assisted $MnMoO_4$ (424.44 F g^{-1}) deliver higher discharge specific capacity than the pristine $MnMoO_4$ nanorods (61.43 F g^{-1}).

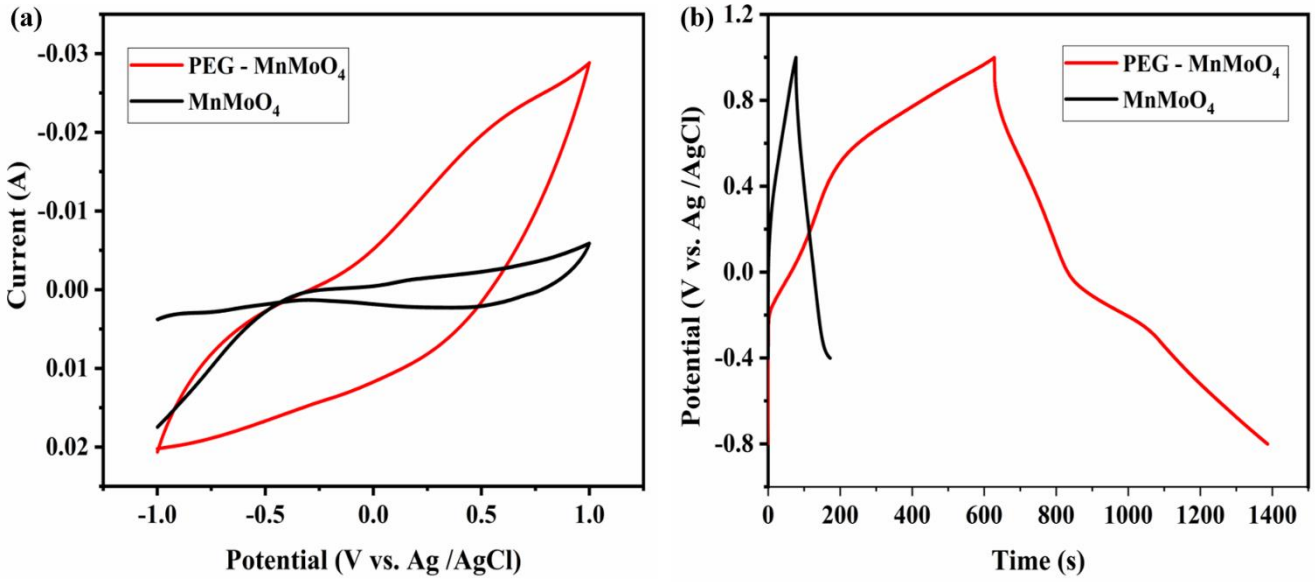

Figure 4. Comparison of electrochemical activity of PEG-$MnMoO_4$ and $MnMoO_4$ nanorods by (a) CV and (b) GCD analysis in 1 M Na_2SO_4 electrolyte.

Although, the CV curves shows the redox behavior for PEG-$MnMoO_4$ nanorods coated Ni-foam electrode. The appearance of oxidation and reduction peak resembles to the anodic process of Mn^{2+} to Mn^{3+} and also cathodic process of Mn^{3+} to Mn^{2+}. Besides, the obtained redox behaviors are almost not changed over the scan rate range of 1-100 mV s^{-1}, however but their peak potentials are little bit shifted to the higher range.

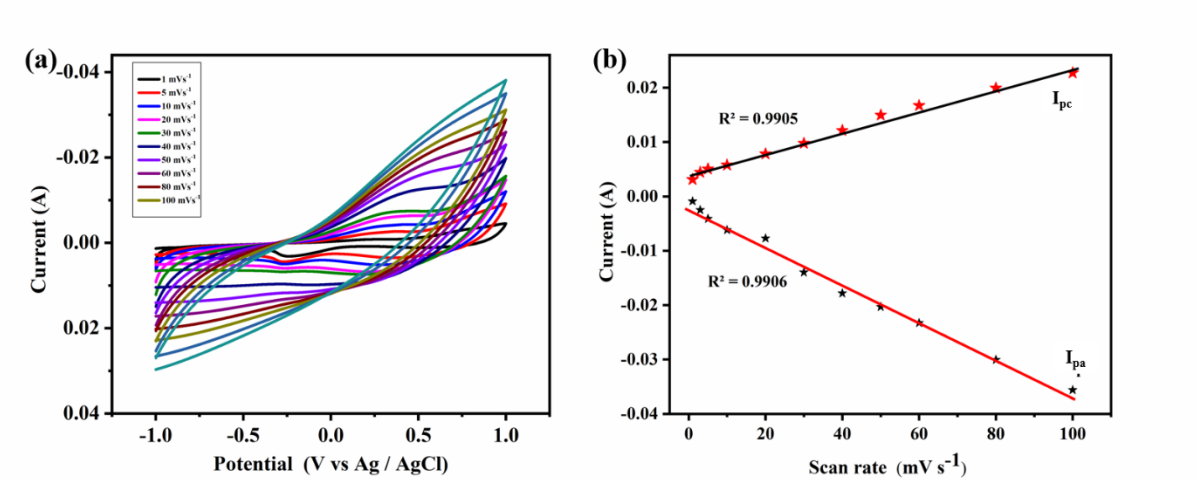

Figure 5. (a) CV curves of PEG-$MnMoO_4$ nanorods electrode at various scan rates such as 1, 5, 10, 20, 30….100 mV s^{-1} in 1 M Na_2SO_4 electrolyte. (b) Linear plot of anodic and cathodic peak current vs. scan rates.

The shape of redox peaks can be deviated over the high scan rates due to the rapid ionic transport where the electrolytes are not fully adsorbed on the $MnMoO_4$ nanorods surface. The plot of peak current versus scan rates shows the typical linear fit of surface controlled reaction process of the materials, suggesting that the electrode of $MnMoO_4$ nanorods is appropriate for good reversibility and high specific capacity achievements. From these results, it can be also identified that the peak currents are increased due to increasing the scan rates, indicates kinetics of the pseudocapacitive behavior of the material. It is also reveals the rates of electronic and ionic transportations are very fast at the PEG-$MnMoO_4$ nanorods coated Ni-foam electrode/electrolyte interfaces. Furthermore, during the CV analysis, the molybdate ions are not involve in these redox process where it may encourage the electrical conductivity of the materials.

GCD analysis was performed using PEG-$MnMoO_4$ nanorods based electrode materials at the potential window of -0.8 to +1.0 V vs. Ag/AgCl in 1 M Na_2SO_4 at different current densities. Fig. 5a shows the typical pseudocapacitive behavior of PEG-$MnMoO_4$ nanorods coated Ni-foam electrode. The specific discharge capacity (C_s) of the material was calculated by using the below equation (5);

$$C_s = \frac{I\Delta t}{m\Delta v}\, Fg^{-1} \qquad (5)$$

Where, I (A) is the discharge current, ΔV is the potential window used in this study, m (g) is the mass of the active material, and Δt (s) is the discharge time. The calculated specific discharge capacities of the PEG-$MnMoO_4$ nanorods coated Ni-foam electrode are of 424, 281, 221, 177 and 138 F g^{-1} at 1, 2, 3, 4 and 5 A g^{-1}, respectively. The result shows that the specific capacities are decreased upon increasing the current densities which is due to the low diffusion rates of the ions into the inner active sites of the materials. According to GCD results, the PEG-$MnMoO_4$ nanorods coated Ni-foam electrode obtained high specific capacity of 424 F g^{-1} at 1 A g^{-1} current density, the value is really higher than the previously reported $MnMoO_4$ electrode materials [3,4,21,24,26-28]. As seen in **Table 1**, it is

observed that the literature report samples have lower specific capacitance than the PEG-$MnMoO_4$ prepared in the present work.

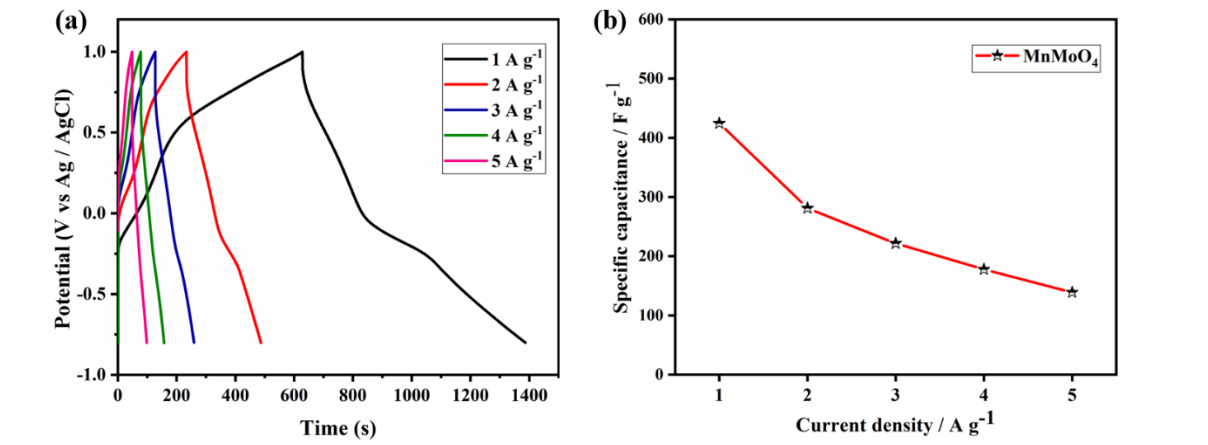

Figure 5. (a) GCD curves of PEG-$MnMoO_4$ nanorods electrode at different current density of 1, 2, 3, 4 and 5 A g^{-1} in 1 M Na_2SO_4 electrolyte. (b) Calibration plot of discharge specific capacity vs. current density.

In summary, a facile synthesis approach is demonstrated to prepare $MnMoO_4$ nanorods by the assistance of PEG surfactant. Uniform and highly crystalline $MnMoO_4$ nanorods were obtained when using PEG surfactant, as compared to without aid of PEG. This obtained unique morphology can improves the electrochemical properties of the binary metal oxide, i.e., $MnMoO_4$, and enhances the energy storage behavior with wide range of potential window.

Table 1. Compare the specific capacity of PEG-$MnMoO_4$ nanorod electrodes with the other reported literatures with respect to synthesis method, electrolyte system and potential window

Material	**Preparation Method**	**Electrolyte**	**ΔV**	**Specific capacity (F g^{-1})**	**Ref.**
$MnMoO_4$	Co-precipitation	2 M NaOH	1	200 (1.6 A g^{-1})	24
$MnMoO_4$	Hydrothermal	1 M Na_2SO_4	2	364 (2 A g^{-1})	27
$MnMoO_4$/$CoMoO_4$	Simple refluxing	2 M NaOH	0.75	~181 (1 A g^{-1})	4
3D α-$MnMoO_4$	Self-assembly	2 M KOH	0.4	562 (1 A g^{-1})	21
$MnMoO_4$	Co-precipitation	2 M KCl	1	~374 (0.2 A g^{-1})	26
$MnMoO_4$	Sonochemical	1 M Na_2SO_4	1	373 (1 A g^{-1})	28
$MnMoO_4$	Sonochemical	2 M NaOH	0.65	168 (1 A g^{-1})	3
PEG-$MnMoO_4$ nanorods	Co-precipitation with surfactant	1 M Na_2SO_4	1.8	424 (1 A g^{-1})	**Present work**

4. CONCLUSION

In this work, PEG-assisted $MnMoO_4$ nanorods has been prepared by using a facile co-precipitation method approach. The electrochemical performance results indicated that the PEG-$MnMoO_4$ nanorods coated Ni-foam electrodes are promising for supercapacitor application. Here, the prepared $MnMoO_4$ materials exhibited a nanorod-like morphology and homogeneous distribution of Mn and Mo element. The high crystallinity of PEG-$MnMoO_4$ nanorods exhibits higher discharge specific capacitance than the pristine $MnMoO_4$ nanorods, the performance was confirmed by typical CV and GCD method. The specific capacitance of 424 F g^{-1} at 1 A g^{-1} was obtained for the as-synthesized PEG-$MnMoO_4$ nanorods coated Ni-foam electrode which is far better than the other $MnMoO_4$ nanorods synthesized by the other methods. Hence, the pseudocapacitive nature of the PEG-$MnMoO_4$ nanorods can be fabricated to asymmetric capacitor electrode for further improve cyclic stability and viability of high power energy storage application.

ACKNOWLEDGEMENTS
The funding was received from the Ministry of Science and Technology, Taiwan (MOST 107-2113-M-027-055-MY3). Mr. Krishnan Venkatesh was sincerely expressed his sincere thanks to professor Chun-Chen Yang, Battery Research Center of Green Energy, Ming Chi University of Technology, New Taipei City, Taiwan for the instrument facilities of this work and also he has gratefully acknowledges the TEEP@Asia Plus for giving him valuable internship program.

References

1. A.D. Jagadale, V.S. Kumbhar, D.S. Dhawale, C.D. Lokhande, *J. Electroanal. Chem*, 704 (2013) 90–95.
2. J.H. Jang, S. Han, T. Hyeon, S.M. Oh, *J. Power Sources*, 123 (2003) 79–85.
3. G.K. Veerasubramani, K. Krishnamoorthy, R. Sivaprakasam, S.J. Kim, *Mater. Chem. Phys*, 147 (2014) 836–842.
4. L.Q. Mai, F. Yang, Y.L. Zhao, X. Xu, L. Xu, Y.Z. Luo, *Nat. Commun*, 2 (2011).
5. Y. Zheng, M. Zhang, P. Gao, *Mater. Res. Bull*, 42 (2007) 1740–1747.
6. H. Cao, N. Wu, Y. Liu, S. Wang, W. Du, J. Liu, *Electrochim. Acta*, 225 (2017) 605–613.
7. H. Li, H. Xuan, J. Gao, T. Liang, X. Han, Y. Guan, J. Yang, P. Han, Y. Du, *Electrochim. Acta*, 312 (2019) 213–223.
8. T. Morishita, Y. Soneda, H. Hatori, M. Inagaki, *Electrochim. Acta*, 52 (2007) 2478–2484.
9. Y. Sato, K. Yomogida, T. Nanaumi, K. Kobayakawa, Y. Ohsawa, M. Kawai, *Electrochem. Solid-State Lett*, 3 (2000) 113–116.
10. M. Ramani, B.S. Haran, R.E. White, B.N. Popov, L. Arsov, *J. Power Sources*, 93 (2001) 209–214.
11. S.K. Meher, G.R. Rao, *J. Phys. Chem. C*, 115 (2011) 15646–15654.
12. K. Xu, R. Zou, W. Li, Q. Liu, T. Wang, J. Yang, Z. Chen, J. Hu, *New J. Chem*, 37 (2013) 4031–4036.
13. S. Chen, J. Zhu, X. Wu, Q. Han, X. Wang, *ACS Nano*, 4 (2010) 2822–2830.
14. X. Cao, B. Zheng, W. Shi, J. Yang, Z. Fan, Z. Luo, X. Rui, B. Chen, Q. Yan, H. Zhang, *Adv. Mater*, 27 (2015) 4695–4701.
15. B. Saravanakumar, S.P. Ramachandran, G. Ravi, V. Ganesh, A. Sakunthala, R. Yuvakkumar, *Appl. Phys. A Mater. Sci. Process*, 125 (2019) 1–11.

16. D. Du, R. Lan, W. Xu, R. Beanland, H. Wang, S. Tao, *J. Mater. Chem. A*, 4 (2016) 17749–17756. Open Access
17. J. V. Kumar, R. Karthik, S.Chen, V. Muthuraj , C. Karuppiah, *Scientific Reports*, 6, (2016) 34149.
18. J. V. Kumar, R. Karthik, S.M. Chen, C. Karuppiah, Y.H. Cheng, Muthuraj. V, *ACS Appl. Mater. Interfaces*, 9, 7 (2017) 6547–6559.
19. R. Karthik, J. V. Kumar, Shen-Ming Chen, K. Seerangan, C Karuppiah, T.W. Chen, V. Muthuraj , 9, 31, (2017) 26582–26592.
20. Y. Zhang, W. dong Xue, H. Yin, D. xu He, R. Zhao, *Compos. Part A Appl. Sci. Manuf*, 107 (2018) 271–281.
21. H. Wang, L. Zhang, X. Tan, C.M.B. Holt, B. Zahiri, B.C. Olsen, D. Mitlin, *J. Phys. Chem. C*, 115 (2011) 17599–17605.
22. L. Wang, L. Yue, X. Zang, H. Zhu, X. Hao, Z. Leng, X. Liu, S. Chen, *CrystEngComm*, 18 (2016) 9286–9291.
23. X. Yan, L. Tian, J. Murowchick, X. Chen, *J. Mater. Chem. A*, 4 (2016) 3683–3688.
24. B. Senthilkumar, R.K. Selvan, D. Meyrick, M. Minakshi, *Int. J. Electrochem. Sci*, 10 (2015) 185–193.
25. M. Minakshi, T. Watcharatharapong, S. Chakraborty, R. Ahuja, *APL Mater*, 6 (2018).
26. H. Wang, Y. Song, J. Zhou, X. Xu, W. Hong, J. Yan, R. Xue, H. Zhao, Y. Liu, J. Gao, *Electrochim. Acta*, 212 (2016) 775–783.
27. D. Ghosh, S. Giri, M. Moniruzzaman, T. Basu, M. Mandal, C.K. Das, *Dalt. Trans*, 43 (2014) 11067–11076.
28. Y. Johnbosco, V. Elumalai, M. Bhagavathiachari, A.S. Samuel, E. Elaiyappillai, P.M. Johnson, *J. Electroanal. Chem*, 797 (2017) 78–88.